Advanced T700/XB3585 UD carbon fibers-reinforced composite

T. HEITZ[a], H. TEODORESCU-DRAGHICESCU[b], S. LACHE[b], A. CHIRU[b], S. VLASE[b,*] M. R. CALIN[c]
[a]*ThyssenKrupp Presta AG, Essanenstrasse 10, FL-9492 Eschen, Lichtenstein*
[b]*Transilvania University of Brasov, Department of Automotives and Mechanical Engineering, 29 Eroilor Blvd, 500036, Brasov, Romania*
[c]*"Horia Hulubei" National Institute for Physics and Nuclear Engineering - IFIN HH, P.O. Box MG-6, 077125, Magurele, Romania*

A new unidirectional Torray T700 carbon fibers-reinforced composite laminate based on Huntsman XB3585 epoxy resin has been developed in Resin Transfer Molding process with applications in the automotive industry. Numerical simulations have been carried out on this type of laminate subjected to off-axis loading systems to determine its most important elastic properties and compared to experimental data. Specimens cut from various plates axial, transverse and at ±45° to the fibers direction have been subjected to tensile and compression tests to determine axial and transverse Young's moduli as well as axial-transverse shear modulus and Poisson ratio. The numerical simulations present close values to those determined experimentally. Stress-strain distributions as well as most common failure modes are presented.

(Received July 24, 2013; accepted May 15, 2014)

Keywords: Carbon fibers, Torray T700, XB3585 epoxy resin, Tensile/compression tests, Resin Transfer Molding

1. Introduction

Fibers-reinforced composite laminates are composed from many laminae, unidirectional reinforced, stacked one of each other on their thickness direction. In this way appear only normal forces (loading in plane) that cause only strains without bending or torsions. The basic hypotheses of this theory are [1]:

- The laminate is thin and one of its dimensions is far bigger than its thickness;
- Between the laminae, there is a perfect bond;
- The strains distribution on the thickness direction of the laminate is linear;
- From the macroscopic point of view, all laminae are homogeneous and behave linear elastic.

If we consider a composite laminate with N laminae with different fibers disposal angles subjected only to normal forces, the elasticity law of the unidirectional reinforced lamina K can be expressed as follows [2], [3]:

$$\begin{bmatrix} \sigma_{xx\,K} \\ \sigma_{yy\,K} \\ \tau_{xy\,K} \end{bmatrix} = \begin{bmatrix} r_{11\,K} & r_{12\,K} & r_{13\,K} \\ r_{12\,K} & r_{22\,K} & r_{23\,K} \\ r_{13\,K} & r_{23\,K} & r_{33\,K} \end{bmatrix} \cdot \begin{bmatrix} \varepsilon_{xx\,K} \\ \varepsilon_{yy\,K} \\ \gamma_{xy\,K} \end{bmatrix}, \quad (1)$$

where r_{ijK} are the transformed rigidities, σ_{xxK} and σ_{yyK} are the medium stresses of the K lamina on the x-axis respective y-axis directions and τ_{xyK} represents the medium shear stress of the K lamina against the global coordinate system *XOY*. The equilibrium equations of the laminate structure are:

$$n_{xx} = \underline{\sigma}_{xx} \cdot t = \sum_{K=1}^{N} \left(\sigma_{xxK} \cdot t_K \right) = \sum_{K=1}^{N} n_{xxK}, \quad (2)$$

$$n_{yy} = \underline{\sigma}_{yy} \cdot t = \sum_{K=1}^{N} \left(\sigma_{yyK} \cdot t_K \right) = \sum_{K=1}^{N} n_{yyK}, \quad (3)$$

$$n_{xy} = \underline{\tau}_{xy} \cdot t = \sum_{K=1}^{N} \left(\tau_{xyK} \cdot t_K \right) = \sum_{K=1}^{N} n_{xyK}, \quad (4)$$

where n_{xx} and n_{yy} are the normal forces against the unit length of the laminate on the *x* respective *y* directions and n_{xy} is the shear force, in plane, on the unit length of the laminate, against the global coordinate system *XOY*. The normal stresses $\underline{\sigma}_{xx}$ and $\underline{\sigma}_{yy}$ on *x* respective *y* directions of the composite laminate, $\underline{\tau}_{xy}$ represents the shear stress of the laminate against the global coordinate system. t_k and t represent the thickness of the *K* lamina respective the lamina thickness, n_{xxK} and n_{yyK} are the normal forces against the unit length of the *K* lamina on the *x* respective *y* directions and n_{xyK} is the shear force, in plane, on the unit length of the *K* lamina, against the global coordinate system *XOY*.

Beside the equilibrium equations it should be determined the geometrical conditions to compute the stresses. For the composite laminates these conditions are: the laminae must be adherent one of each other and all laminae bear, in a specific point, the same strains ε_{xx}, ε_{yy}, γ_{xy} as the whole laminate. Thus:

$$\varepsilon_{xxK} = \varepsilon_{xx}, \quad \varepsilon_{yyK} = \varepsilon_{yy}, \quad \gamma_{xyK} = \gamma_{xy}, \tag{5}$$

for all K laminae, $K = 1 \ldots N$. With equations (1) – (5), the elasticity law of the composite laminate can be obtained:

$$\begin{bmatrix} \sigma_{xx} \\ \sigma_{yy} \\ \tau_{xy} \end{bmatrix} = \begin{bmatrix} \sum_{K=1}^{N}\left(r_{11K}\cdot\frac{t_K}{t}\right) & \sum_{K=1}^{N}\left(r_{12K}\cdot\frac{t_K}{t}\right) & \sum_{K=1}^{N}\left(r_{13K}\cdot\frac{t_K}{t}\right) \\ \sum_{K=1}^{N}\left(r_{12K}\cdot\frac{t_K}{t}\right) & \sum_{K=1}^{N}\left(r_{22K}\cdot\frac{t_K}{t}\right) & \sum_{K=1}^{N}\left(r_{23K}\cdot\frac{t_K}{t}\right) \\ \sum_{K=1}^{N}\left(r_{13K}\cdot\frac{t_K}{t}\right) & \sum_{K=1}^{N}\left(r_{23K}\cdot\frac{t_K}{t}\right) & \sum_{K=1}^{N}\left(r_{33K}\cdot\frac{t_K}{t}\right) \end{bmatrix} \cdot \begin{bmatrix} \varepsilon_{xx} \\ \varepsilon_{yy} \\ \gamma_{xy} \end{bmatrix}, \tag{6}$$

in addition, from these relations we can recognize the rigidities $\underline{r}_{ij}$ of the composite laminate:

$$\underline{r}_{ij} = \sum_{K=1}^{N}\left(r_{ijK}\cdot\frac{t_K}{t}\right). \tag{7}$$

In these conditions, the elasticity law of the laminate becomes:

$$\begin{bmatrix} \sigma_{xx} \\ \sigma_{yy} \\ \tau_{xy} \end{bmatrix} = \begin{bmatrix} \underline{r}_{11} & \underline{r}_{12} & \underline{r}_{13} \\ \underline{r}_{12} & \underline{r}_{22} & \underline{r}_{23} \\ \underline{r}_{13} & \underline{r}_{23} & \underline{r}_{33} \end{bmatrix} \cdot \begin{bmatrix} \varepsilon_{xx} \\ \varepsilon_{yy} \\ \gamma_{xy} \end{bmatrix}, \tag{8}$$

where $\underline{r}_{ij}$ are functions of the basic elasticity properties of each lamina: $E_{\parallel K}$, $E_{\perp K}$, $\upsilon_{\perp\parallel K}$, $G_{\#K}$ and of the fibers disposal angle α_K.

The basic elasticity properties of the unidirectional reinforced lamina are presented below [4], [5], and [6]:

$$E_{II} = E_F \cdot \varphi + E_M \cdot (1-\varphi), \tag{9}$$

$$\upsilon_{\perp II} = \varphi \cdot \upsilon_F + (1-\varphi)\cdot \upsilon_M, \tag{10}$$

$$E_{\perp} = \frac{E_M}{1-\upsilon_M^2} \cdot \frac{1+0{,}85\cdot\varphi^2}{(1-\varphi)^{1{,}25} + \frac{\varphi\cdot E_M}{(1-\upsilon_M^2)\cdot E_F}}, \tag{11}$$

$$\upsilon_{II\perp} = \upsilon_{\perp II} \cdot \frac{E_{\perp}}{E_{II}}, \tag{12}$$

$$G_{\#} = G_M \cdot \frac{1+0{,}6\cdot\varphi^{0{,}5}}{(1-\varphi)^{1{,}25} + \varphi\cdot\frac{G_M}{G_F}}. \tag{13}$$

Analogue to the stresses, an analysis of the strains can be accomplished. From the relation (8), the strains ε_{xx}, ε_{yy}, γ_{xy} can be computed. The strains of the laminae $\varepsilon_{\parallel K}$, $\varepsilon_{\perp K}$, $\gamma_{\#K}$ results through transformation. Finally, from the transformed strains can be computed the stresses in the individual laminae of the composite laminate:

$$\sigma_{IIK} = \frac{E_{IIK}}{1-\upsilon_{\perp IIK}\cdot\upsilon_{II\perp K}}\cdot\varepsilon_{IIK} + \frac{\upsilon_{\perp IIK}\cdot E_{\perp K}}{1-\upsilon_{\perp IIK}\cdot\upsilon_{II\perp K}}\cdot\varepsilon_{\perp K}, \tag{14}$$

$$\sigma_{\perp K} = \frac{\upsilon_{\perp IIK}\cdot E_{\perp K}}{1-\upsilon_{\perp IIK}\cdot\upsilon_{II\perp K}}\cdot\varepsilon_{IIK} + \frac{E_{\perp K}}{1-\upsilon_{\perp IIK}\cdot\upsilon_{II\perp K}}\cdot\varepsilon_{\perp K}, \tag{15}$$

$$\tau_{\#K} = G_{\#}\cdot\gamma_{\#}. \tag{16}$$

To make a break prediction of the individual laminae, a failure criterion must be used [7-10].

2. Behavior of the carbon fibers Torray T700

In order to characterize the carbon fibers of type Torray T700, some unidirectional fibers-reinforced plates have been developed using following compounds:

- Resin: Huntsman XB 3585;
- Hardener: Huntsman XB 3458;
- Carbon fibers: Torray T700.

The plates have been manufactured in the Resin Transfer Molding (RTM) process. A 51% fibers volume fraction and 2 mm thickness have been reached. More sophisticated method are presented in [11],[12].

To determine the most important elastic properties of Torray T700/XB3585 unidirectional carbon fibers-reinforced composite laminate, like E_x and E_y Youn's moduli, υ_{xy} Poisson ratio and G_{xy} shear modulus, various specimens have been cut along, transverse and at ±45° to the fibers direction with respect to following standards: EN ISO 527-4, DIN 65466 and EN ISO 14126.

Following plates, specimens dimensions, fibers orientations and standards have been used:

1. Plate TKP2-1 (dimensions: 300 x 300 mm; specimens dimensions: 250 x 10 x 2 mm; 10 specimens cut along fibers direction according to EN ISO 527-4 and subjected to tensile tests);
2. Plate TKP1-2 (dimensions: 300 x 300 mm; specimens dimensions: 250 x 25 x 2 mm; 10 specimens cut transverse to fibers direction according to EN ISO 527-4 and subjected to tensile tests);
3. Plate TKP1-3 (dimensions: 300 x 300 mm; specimens dimensions: 250 x 16 x 2 mm; 10 specimens with ±45° fibers orientation and cut according to DIN 65466, subjected to tensile tests);
4. Plate TKP1-4 (dimensions: 300 x 300 mm; specimens dimensions: 110 x 10 x 4 mm; 10 specimens cut along fibers and 10 specimens cut transverse to fibers direction according to EN ISO 14126 and subjected to compression tests).

The plates have been carefully checked in terms of quality by taking micrographs to see if the material's microstructure present voids and a good bond between matrix and fibers.

The specimens have been fixed in grips and hydraulically loaded. Specific speed tests according to standards have been carried out.

Load-extension distributions have been plotted using the hydraulic cylinder of the materials testing machine (Fig. 1). In addition to this, the measurement of strains by means of a laser extensometer of Fiedler Optoelectronics GmbH company have been carrid out. Analogue, the measured strains have been sent to the control of the hydraulic cylinder and time recorded at Kaiserslautern University, Germany.

Fig. 1. The experimental set-up

3. Results

The experimental data have been smoothed using an average method. In case of plate TKP2-1 (specimens cut along fibers direction), following parameters have been determined in simple tensile tests (Table 1). An example of stress-strain distribution is presented in Fig. 2 as well as typical break (Fig. 3).

Table 1. Tensile tests of specimens from plate TKP2-1.

T700 CFRP	Young's modulus [MPa]	Break strength [MPa]	Strain at break [%]	Poisson ratio
Mean value	98879	1782	1.75	0.28
Standard deviation	8211	282	0.18	0.096
Coeff. of variance	8.3%	15.8%	10.3%	35%

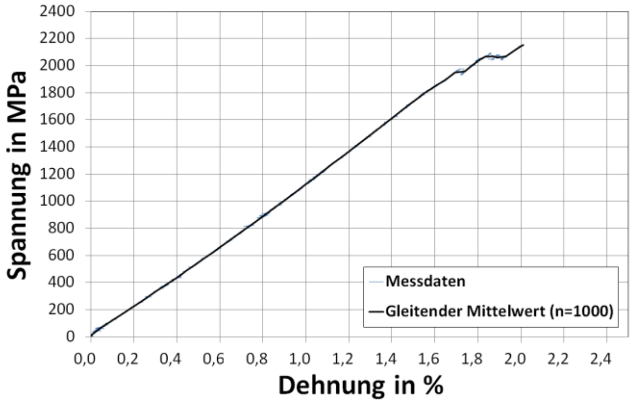

Fig. 2. Stress-strain distribution of a specimen cut from plate TKP2-1 (along fibers direction).

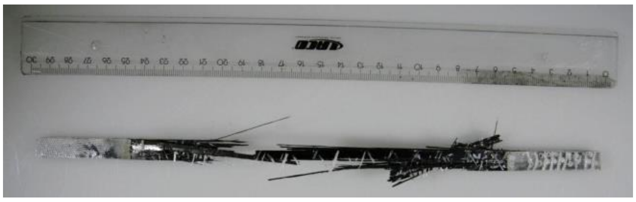

Fig. 3. Typical break in form of a brush of specimens cut from plate TKP2-1.

In case of plate TKP1-2 in which the specimens have been cut transverse to the fibers direction, the tensile tests features are presented in Table 2. A typically stress-strain distribution and common failure are shown in Figs. 4-5.

Table 2. Tensile tests features of specimens cut from plate TKP1-2.

T700 CFRP	Young's modulus [MPa]	Break strength [MPa]	Strain at break [%]
Mean value	7137	46	0.66
Standard deviation	716	4.9	0.060
Coefficient of variance	10%	10.7%	9.2%

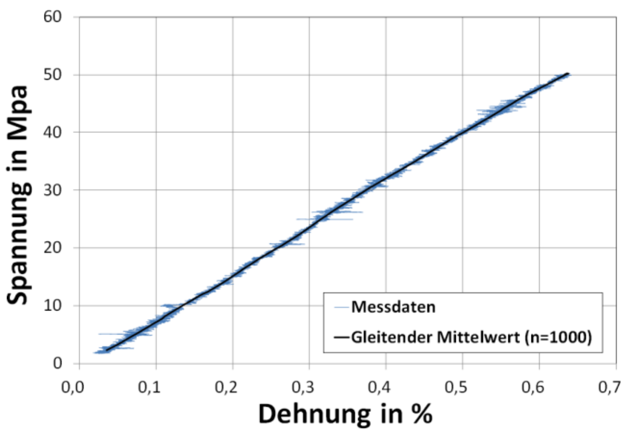

Fig. 4. Stress-strain distribution of a specimen cut from plate TKP1-2 (transverse to fibers direction).

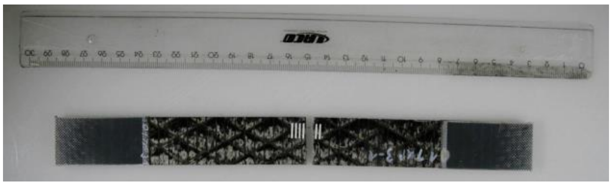

Fig. 5. Common break in case of specimens cut from plate TKP1-2.

To determine the shear modulus of T700/XB3585 unidirectional carbon fibers-reinforced composite, ten specimens have been cut from plate TKP1-3 and subjected to tensile tests until break. The main features of these tests are presented in Table 3. Common stress-strain behavior and failure mode are visualized in Figs. 6-7.

Table 3. Tensile tests of specimens from plate TKP1-3.

T700 CFRP	Shear modulus [MPa]	Shear strength [MPa]	Shear strain at break [%]
Mean value	5619	121	2.1565
Standard deviation	805	2.1	0.51
Coeff. of variance	14.3%	1.7%	23.6%

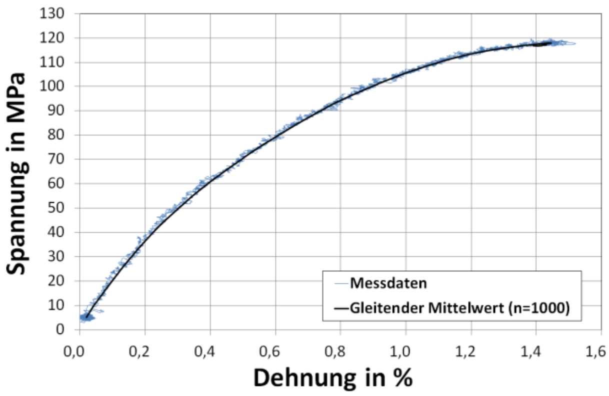

Fig. 6. Stress-strain distribution of a specimen cut from plate TKP1-3 (±45° fibers orientation) to determine the shear modulus.

Fig. 7. Usual failure in case of specimens cut with ±45° fibers orientation and cut according to DIN65466 from plate TKP1-3.

From plate TKP1-4, ten specimens have been cut along fibers direction and ten transverse to the fibers direction to determine the most important mechanical properties in compression tests. The main features of compression tests in case of specimens cut along fibers direction are presented in Table 4, typical stress-strain distribution and common failure are shown in Figs. 8-9.

Table 4. Compression tests of specimens cut from plate TKP1-4 (along fibers direction).

T700 CFRP	Young's modulus [MPa]	Strength at break [MPa]	Strain at break [%]
Mean value	105974	607	0.9133
Standard deviation	24975	39.5	0.23502
Coeff. Of variance	23.6%	6.7%	25.7%

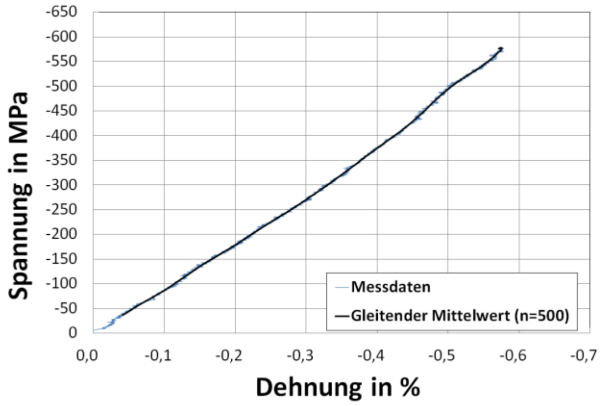

Fig. 8. Stress-strain behavior of specimens cut along fibers direction from plate TKP1-4 subjected to compression tests.

Fig. 9. Common failure of specimens cut along fibers direction from plate TKP1-4 subjected to compression tests.

In case of specimens cut transverse to fibers direction from plate TKP1-4 and subjected to compression tests, the main mechanical properties are presented in Table 5. Stress-strain distribution and usual failure are visualized in Figs. 10-11.

Table 5. Compression tests of specimens cut from plate TKP1-4 (transverse to fibers direction).

T700 CFRP	Young's modulus [MPa]	Strength at break [MPa]	Strain at break [%]
Mean value	8265	185	3.6159
Standard deviation	1328.6	8.5	1.03542
Coeff. Of variance	16.1%	4.6%	28.6%

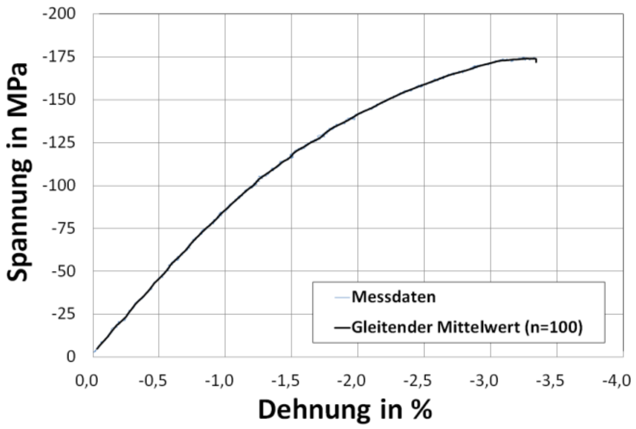

Fig. 10. Stress-strain behavior of specimens cut transverse to fibers direction from plate TKP1-4 subjected to compression tests.

Fig. 11. Common failure of specimens cut transverse to fibers direction from plate TKP1-4 subjected to compression tests.

Some numerical simulations have been carried out based on the theoretical approach presented in reference [13] to determine the elastic properties of T700/XB3585 unidirectional carbon fibers-reinforced composite subjected to off-axis loading systems. Following input data have been used:

- Fibers volume fraction: 0.51;
- Laminate thickness: 2 mm;
- Off-axis loading systems: between 0°and 90°;
- Fibers Young's modulus (axial direction): 230 GPa;
- Fibers Young's modulus (transverse direction): 3.23 GPa;
- Matrix Young's modulus: 3 GPa;
- Fibers shear modulus (axial-transverse direction): 98 MPa;
- Matrix shear modulus (axial-transverse direction): 1.15 GPa;
- Fibers axial-transverse Poisson ratio: 0.28;
- Matrix Poisson ratio: 0.3.

Young's moduli E_x and E_y as well as shear modulus G_{xy} distributions of T700/XB3585 unidirectional carbon fibers-reinforced composite laminate subjected to off-axis loading systems between 0° and 90° are presented in Figs. 12-14.

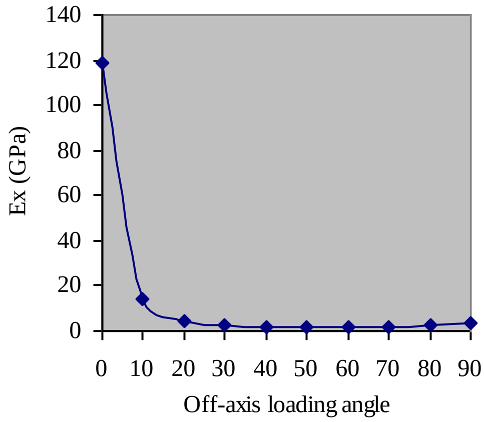

Fig. 12. Numerical simulation of Young's modulus (E_x).

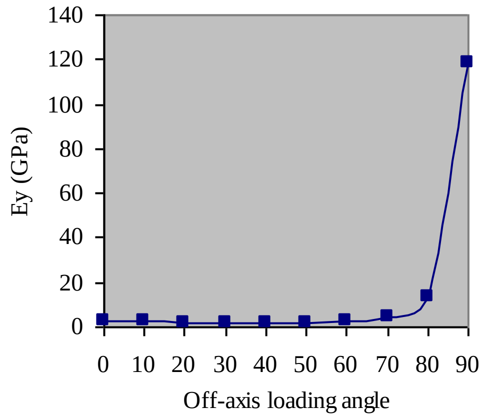

Fig. 13. Numerical simulation of Young's modulus (E_y).

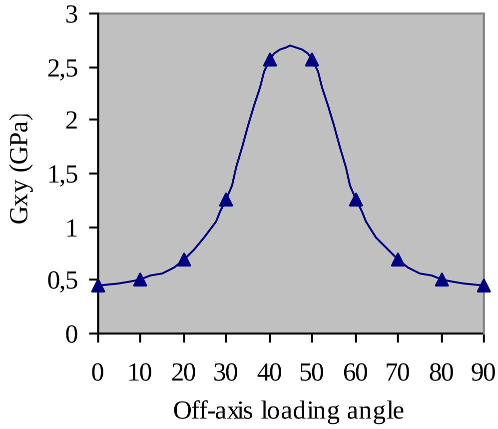

Fig. 14. Numerical simulation of shear modulus (G_{xy})

4. Discussion

From presented experimental results, a strong anisotropy can be noticed between specimens cut along fibers direction and those cut transverse to the fibers direction subjected to tensile and compression tests (see Figs. 2, 4, 8 and 10). An outstanding maximum load at break of 39 kN has been reached in case of specimens cut from plate TKP2-1 along fibers direction and subjected to tensile tests. Regarding the numerical simulations carried out on T700/XB3585 unidirectional carbon fibers-reinforced composite laminate subjected to off-axis loading systems between 0° and 90°, the Young's moduli E_x and E_y as well as the shear modulus G_{xy} present close values with those determined in tensile tests (Figs. 15-17).

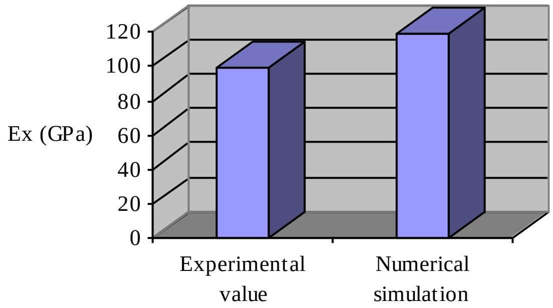

Fig. 15. Comparisson between Young's modulus E_x determined experimentally and by numerical simulation.

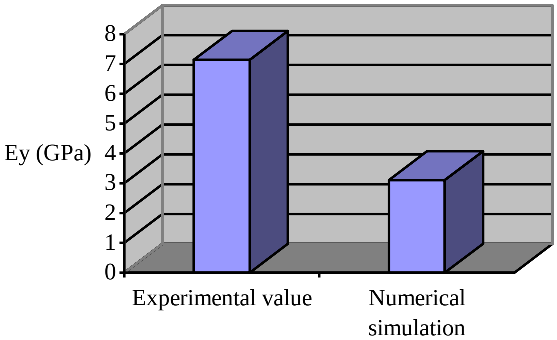

Fig. 16. Comparisson between Young's modulus E_y determined experimentally and by numerical simulation.

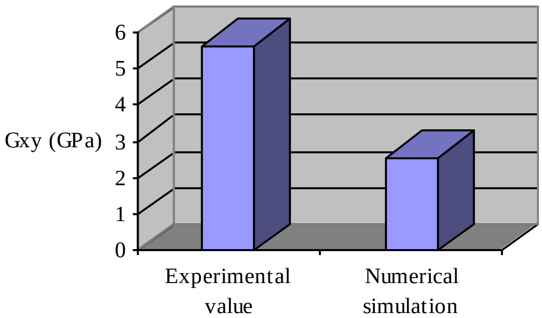

Fig. 17. Comparisson between shear modulus G_{xy} determined experimentally and by numerical simulation.

5. Conclusions

The new unidirectional Torray T700 carbon fibers-reinforced composite laminate based on Huntsman XB3585 epoxy resin developed in Resin Transfer Molding process presents excellent mechanical properties especially along fibers direction. These properties recommend this outstanding composite material to be used as replacement material in the automotive industry, for instance in case of steering collumns.

Tensile-shear interactions lead to distortions and local micro-structural damage and failure, so to obtain equal stiffness in all off-axis loading systems, a composite laminate have to present balanced angle plies. These tensile-shear interactions are also present in composite laminates but does not occur if the loading system is applied along the main axes of a single lamina or if a laminate is balanced. Under off-axis loading systems, normal stresses produce shear strains and normal strains. Shear stresses exhibit normal strains as well as shear strains.

References

[1] H. Schürmann, Konstruiren mit Faser-Kunststoff-Verbunden, Springer (2005).
[2] H. Teodorescu-Draghicescu, S. Vlase, L. Scutaru, L. Serbina, M.R. Calin, Optoelectron. Adv. Mater. – Rapid Comm., **5**(3), 273 (2011).
[3] S. Vlase, H. Teodorescu-Draghicescu, D. L. Motoc, M. L. Scutaru, L. Serbina, M. R. Calin, Optoelectron. Adv. Mater. – Rapid Comm., **5**(4), 419 (2011).
[4] S. Vlase, H. Teodorescu-Draghicescu, M. R. Calin, L. Serbina, Optoelectron. Adv. Mater. – Rapid Comm., **5**(4), 424 (2011).
[5] H. Teodorescu-Draghicescu, A. Stanciu, S. Vlase, L Scutaru, M. R. Calin, L. Serbia, Optoelectron. Adv. Mater. – Rapid Comm. **5**(7), 782 (2011).
[6] H. Teodorescu-Draghicescu, S. Vlase, Computational Materials Science, **50**(4), February (2011).
[7] A. Stanciu, H. Teodorescu-Draghicescu, S. Vlase, M.L. Scutaru, M. R. Calin, Optoelectron. Adv. Mater. – Rapid Comm., **6**(3-4), 495 (2012).
[8] S. Vlase, H. Teodorescu-Draghicescu, M.R. Calin, M.L. Scutaru, J. Optoelectron. Adv. Mater., **14**(7-8), 658 (2012).
[9] H. Teodorescu-Draghicescu, M. L. Scutaru, D. Rosu, M. R. Calin, P. Grigore, J. Optoelectron. Adv. Mater., **15**(3-4), 199 (2013).
[10] A. Modrea, S. Vlase, H. Teodorescu-Draghicescu, M. Mihalcica, M. R. Calin, C. Astalos, Optoelectron. Adv. Mater. – Rapid Comm., **7**(5-6), 452 (2013).
[11] I. Szava, R. D. Necula, B. Galfi, D. Szava, I. Samota, New Methods in Bio-mechanical Experimental Investigations. Proceedings of the 50the Annual Conference on Experimental Stress Analysis, p. 449, (2012).
[12] C. Itu, F. Dogaru, M. Baba, Dynamic con-rod analysis for different type of materials based on virtual simulation., International Conference on Materials Science and Engineering BRAMAT 2007, Brasov, Romania, ISSN 1223 – 9631.
[13] D. Hull, T. W. Clyne, An Introduction to Composite Materials, CUP (1996).

*Corresponding author: svlase@unitbv.ro